

PREPARATION AND ADSORPTION STUDIES OF PHOSPHORYLATED CELLULOSE MICROSPHERES

DANA M. SUFLET, IRINA POPESCU and IRINA M. PELIN

*Petru Poni Institute of Macromolecular Chemistry, 41A, Grigore Ghica Voda Alley,
700487, Iasi, Romania*

✉ *Corresponding author: D. M. Suflet, dsuflet@icmpp.ro*

Received November 1, 2015

New anionic microspheres based on monobasic cellulose phosphate were obtained by chemical cross-linking with epichlorohydrin, using the water-in-oil inverse emulsion technique. SEM and FTIR spectroscopy were used to analyse the morphology and chemical structure of the microspheres. The main characteristics, such as the wrack density, swelling degree, and the exchange capacity, were investigated. These new anionic microspheres could be used as potential adsorption materials. In this respect, the adsorption capacity of methylene blue and rhodamine 6G taken as models was studied. The Langmuir model fitted the adsorption data better than the Freundlich model. Moreover, the kinetic adsorption data were in close agreement with the pseudo-second order kinetic model, which supported the assumption that dye adsorption occurs by physical interactions. Intra-particle and Boyd's models suggested that the intra-particle diffusion was not only a rate-controlling process, but also the film diffusion process played some role in the adsorption on the monobasic cellulose phosphate microspheres.

Keywords: cellulose phosphate, microspheres, adsorption kinetics

INTRODUCTION

Dyes are widely used in industries, such as textiles, leather, paper, printing, plastics, pharmaceutical, cosmetic, food, etc. Some dyes and their degradation products may be toxic, allergenic, mutagenic, and carcinogenic.¹ Consequently, they are important sources of water pollution and their removal becomes a major problem for environmental management. Amongst numerous techniques of dye removal, adsorption is the most used and the most efficient.² The use of adsorbents based on polysaccharides and their derivatives is a big advantage due to their renewability, biodegradability and non-toxicity.³⁻⁵ Amongst polysaccharides, cellulose is the most abundant natural polymer and thus one of the most potential resources to replace the adsorbents based on synthetic polymers. In this respect, cellulose and its derivatives can be used to obtain cellulosic-based materials, which could be employed as cheap dye adsorbents.⁶⁻¹¹ To our knowledge, the obtaining of adsorbent materials based on monobasic cellulose phosphate (PCell) has not been reported in the literature. Compared to other

cellulose derivatives, cellulose phosphates possess the advantages of low cost, easy preparation and low toxicity.^{12,13} From this point of view, in this paper, new anionic microparticles based on PCell were obtained by chemical cross-linking with epichlorohydrin using the water-in-oil inverse emulsion technique. The morphology and size distribution of microparticles were analysed by scanning electron microscopy and the chemical structure was confirmed by FTIR spectroscopy. The main characteristics of these new microspheres, such as the swelling degree in various pH solutions and the exchange capacity, were determined. In order to use the microspheres as adsorption materials, the adsorption capacity of cationic dyes (methylene blue and rhodamine 6G were selected as model compounds) was studied using the batch-adsorption technique. The influence of the microparticles dosage, pH, and initial dye concentration on the microparticles adsorption capacity was followed at equilibrium. Experimental data were examined using several isotherm models in order to establish the most appropriate model to design the adsorption of

ionic microspheres and the adsorption kinetics were fitted in order to obtain a better understanding of the dye adsorption mechanism onto this novel adsorbent.

EXPERIMENTAL

Materials

The monobasic cellulose phosphate (PCell, with a degree of substitution of about 0.6) was synthesised in our laboratory.¹⁴ Epichlorohydrin (ECH), 1,2-dichloroethane, cellulose acetate butyrate (CAB), sodium hydroxide, acetone, and ethylic ether (Sigma-Aldrich, Germany) were used as received. The methylene blue (MB) and rhodamine 6G (R6G) were purchased from Sigma-Aldrich, Germany, and taken as model dyes. All experiments were performed using distilled water, with 5 μ S/cm conductivity.

Synthesis of microspheres

Monobasic cellulose phosphate microspheres (PCellMS) were prepared by chemical cross-linking with ECH using the water-in-oil (w/o) inverse (mini)emulsion. Briefly, 2 g of monobasic cellulose phosphate was dissolved in 0.5 M NaOH aqueous solution (40 ml). The solution was poured in 100 mL of dispersion medium (1,2-dichloroethane) in which 3 g of CAB (as dispersion agent) was dissolved. The w/o emulsion was stirred for 1 h at 700 rpm for obtaining a stable dispersion, then 10 mL of ECH was added and the cross-linking reaction was carried out at 55 °C for 48 h. The cross-linked microparticles were recovered by filtration and then washed for removing residuals in the following order: 1,2-dichloroethane, acetone, twice-distilled water, acetone, and ethylic ether. Finally, the microspheres were completely dried by overnight exposure to 60 °C, under vacuum.

Analysis and characterization of cellulose phosphate microspheres

The microspheres morphology and particle size were evaluated by scanning electron microscopy (SEM, Quanta 200, FEI). The wrack density was determined by weighing a volume of 1 mL of dried microspheres placed in a graduated cylinder (i.d. = 11 mm). The swelling degree was evaluated using the centrifugation method¹⁵ as follows: the dry microspheres (20 mg) were placed into stainless steel baskets that have a sieve and a filter paper at the bottom, and the baskets were immersed into water with a certain pH (adjusted with NaOH or HCl solutions). After the swelling of the microspheres (24 hours), the baskets were centrifuged at 1000 rpm for 15 minutes, when only the swelled microparticles remained, without excess solvent. The water retained into the microparticles, measured by weighing, was reported to the amount of dry microspheres.

The exchange capacity of the microspheres (EC) was determined by the titration method, using a

Metrohm all purposes 716 DMS Titrino apparatus equipped with a 6.0203.100 combined electrode. Firstly, 100 mg of ionic microspheres were swollen in 20 mL water for 12 h. After that, an excess of 0.1N HCl solution (5 mL) was added and maintained for 5 h, under gentle stirring. The supernatant solution was collected and titrated with a 0.1N NaOH solution. The exchange capacity (EC) was expressed as meq. phosphoric groups/g dried microspheres.

Dye adsorption

Adsorption studies were performed at room temperature using the batch technique. The dye concentration was determined spectrophotometrically using a UV-Vis spectrophotometer (Thermo Fisher Scientific Evolution 201, USA) by using a linear calibration plot established for MB and R6G at 663 nm and 526 nm, respectively.

Effect of pH and initial dye concentration

The effect of the initial pH on the adsorption capacity of PCellMS was investigated as follows: 20 mg of PCellMS were added to each dye solution (20 mL; 100 mg/L) at ambient temperature and shaken at 200 rpm for 24 h. The initial solution pH (between 2 to 11) was adjusted by adding 0.1N NaOH or 0.1 N HCl. The dye solutions were collected after 24 h and assayed by UV-Vis spectroscopy.

The effect of dye concentration on the adsorption capacity of microspheres was also investigated as follows: 20 mg microspheres were added to each dye solution (20 mL; 10-500 mg/L) and allowed to interact for 24 h under gentle shaking (200 rpm) at room temperature. The final dye concentrations were determined by UV-Vis spectroscopy.

The amount of dye adsorbed by the microspheres at equilibrium (q_e) was calculated from the difference between the initial concentration of dye and the dye concentration in the supernatant after adsorption (Eq. (1)):

$$q_e = \frac{V(C_0 - C_f)}{m} \quad (1)$$

where C_0 and C_f are the initial and final dye concentration (mg/L), V is the volume of the dye solution (L), and m is the mass of the adsorbent used (g). The amount of adsorbed dye onto microspheres was also calculated as percentage of removal (R , %) according to Eq. (2):

$$R(\%) = \frac{100(C_0 - C_f)}{C_0} \quad (2)$$

Equilibrium adsorption

For equilibrium dye adsorption experiments, fixed amounts of the PCellMS (20 mg) were equilibrated in 20 mL of aqueous dye solutions of varying concentrations. The residual equilibrium dye concentration in the solutions was calculated from UV-

Vis data. The Langmuir isotherm model described by Eq. (3) was linearized Eq. (4) as:

$$q_e = \frac{K_L C_e}{1 + a_L C_e} \quad (3)$$

$$\frac{C_e}{q_e} = \frac{1}{K_L} + \frac{a_L}{K_L} C_e \quad (4)$$

where q_e – the solid phase adsorbate concentration at equilibrium (mg/g), C_e – the aqueous phase adsorbate concentration at equilibrium (mg/L), and K_L (L/g) and a_L (L/mg) are the Langmuir isotherm constants. The plot of C_e/q_e vs. C_e gives a straight line with the slope a_L/K_L and intercept $1/K_L$. The maximum adsorption capacity of the adsorbent (q_m , mg/g) corresponds to K_L/a_L . Hereby, a dimensionless constant commonly known as separation factor (R_L), used to predict the adsorption behaviour of dyes, can be represented as:

$$R_L = \frac{1}{1 + a_L C_0} \quad (5)$$

where K_L (L/mg) refers to the Langmuir constant related to the energy of adsorption and C_0 represents the initial dye concentration (mg/L). In this context, the lower R_L value means that adsorption is more favourable. In a more complex explanation, the R_L value indicates the adsorption nature to be either favourable ($0 < R_L < 1$), irreversible ($R_L = 0$), linear ($R_L = 1$), or unfavourable ($R_L > 1$).¹⁶

The Freundlich isotherm is an empirical model describing the non-ideal and reversible adsorption, not restricted to the formation of monolayer. This model is widely applied in heterogeneous systems especially for organic compounds or highly interactive species, and it is described by Eq. (6):

$$q_e = K_F C_e^{1/n_F} \quad (6)$$

where q_e – the solid phase adsorbate concentration at equilibrium (mg/g), C_e – the aqueous phase adsorbate concentration at equilibrium (mg/L), K_F – the Freundlich constant (L/g) being of the extent of adsorption, and $1/n_F$ – the heterogeneity factor being an indicator of adsorption effectiveness and the deviation from linearity of the adsorption process. The $1/n_F$ value ranges between 0 and 1 is a measure of adsorption intensity or surface heterogeneity, becoming more heterogeneous as its value gets closer to zero. The Freundlich isotherm in Eq. (6) can be linearized, as shown in Eq. (7):

$$\ln q_e = \ln K_F + \frac{1}{n_F} \ln C_e \quad (7)$$

The Dubinin-Radushkevich isotherm is an empirical model initially conceived for the adsorption of subcritical vapours onto micropore solids, following a pore filling mechanism.¹⁷ It is generally applied to express the adsorption mechanism with a Gaussian energy distribution onto heterogeneous surface.

$$q_e = q_s e^{-k_{DR} \varepsilon^2} \quad (8)$$

$$\varepsilon = RT \ln\left(1 + \frac{1}{C_e}\right) \quad (9)$$

$$E = \frac{1}{(2k_{DR})^{1/2}} \quad (10)$$

where q_e is the solid phase adsorbate concentration at equilibrium (mg/g), q_s is the maximum adsorption capacity of dye ion (mg/g), k_{DR} is denoted as the D-R isotherm constant (mol^2/kJ^2), and the parameter ε can be correlated as in Eq. 9, where R , T and C_e represent the gas constant (8.314 J/mol·K), absolute temperature (K), and adsorbate equilibrium concentration (mg/L), respectively. The free energy of adsorption, E (kJ/mol), is defined as the free energy when one mole of ion is transferred to the surface of a solid from infinity in solution (Eq. 10). The value of E is used to estimate the adsorption type. The magnitude of E , less than 8 kJ/mol, indicates that the adsorption process is physical in nature, while the range of value 8-16 kJ/mol indicates that the process of adsorption proceeds by ion exchange. Chemisorption is characterized by E values higher than 40 kJ/mol.

The Temkin isotherm equation assumes that the adsorption is characterized by a uniform distribution of binding energy, up to some maximum binding energy, and that the heat of adsorption of all the molecules in the layer would decrease linearly with converge due to adsorbent-adsorbate interactions. The Temkin isotherm (11) can be linearized as shown in Eq. (12):

$$q_e = \frac{RT}{b_T} \ln(a_T C_e) \quad (11)$$

$$q_e = \frac{RT}{b_T} \ln a_T + \frac{RT}{b_T} \ln C_e \quad (12)$$

where b_T is the Temkin constant related to the heat of adsorption (kJ/mol) and a_T is the equilibrium binding constant corresponding to the maximum binding energy (L/mg), R is the gas constant (8.31 J/mol K), and T (K) is the absolute temperature.

Adsorption kinetics

In order to evaluate the effect of control time on the dye adsorption capacity of PCellMS, samples of 20 mg microparticles were immersed in 20 mL of dye solution (100-500 mg/L) for different contact durations (up to 26 h) and shaken at 200 rpm. The dye concentration in the supernatant was determined by UV-Vis spectroscopy. The experimental data were analysed by several kinetics models: Lagergren rate known as pseudo-first-order kinetics model (Eq. 13), the pseudo-second-order (Eq. 14), intra-particle diffusion, Eq. 15, and Boyd's (Eq. 16) models were applied in order to investigate the diffusion mechanism.^{18,19}

$$\log(q_e - q_t) = \log q_e - \frac{k_1}{2.303} t \quad (13)$$

$$\frac{t}{q_t} = \frac{1}{k_2 q_e^2} + \frac{1}{q_e} t \quad (14)$$

$$q_t = k_i t^{1/2} + I \quad (15)$$

$$B_t = -0.4977 - \ln\left(1 - \frac{q_t}{q_e}\right) \quad (16)$$

where q_t (mg/g) and q_e (mg/g) indicate the dye adsorbed amount at time t (min) and equilibrium, respectively, k_1 , k_2 , and k_i are the pseudo-first order rate constant (min^{-1}), the pseudo-second order rate constant ($\text{g/mg}\cdot\text{min}$), and the intra-particle diffusion rate constant ($\text{mg/g}\cdot\text{min}^{1/2}$) for the adsorption process respectively; t is time (min), and I is the intercept of the y axis, which gives an idea about the thickness of the boundary layer. The B_t is a mathematical function that represents the fraction of adsorbate adsorbed at different times and it is used to identify whether external transport or intra-particle transport controls the rate of sorption. The Boyd's model assumes that the bound layer surrounding the adsorbent particle is the main resistance to diffusion.

RESULTS AND DISCUSSION

Preparation and characterization of microspheres

The microspheres based on PCell were synthesised by chemical cross-linking with ECH using the w/o inverse emulsion technique (Scheme 1). The chemical structure of PCellMS was confirmed by FTIR spectrometry (Fig. 1). In the FTIR spectrum of PCellMS, the following characteristic bands were observed: a large band at 3349 cm^{-1} corresponding to the OH groups; a band at 2899 cm^{-1} attributed to the CH_2 groups; the band at 1653 cm^{-1} owing to the associated water; the bands between 1432 and 1282 cm^{-1}

corresponding to CH_2 and C-OH from the glucosidic units; a large band at $1164\text{-}1031\text{ cm}^{-1}$ attributed to C-O-C from the glucosidic units, and a band at 896 cm^{-1} for the $\beta\text{-D}$ -glucosidic bonds. In addition, the bands of the phosphate groups could be observed in the spectrum of PCellMS: $2404\text{-}2362\text{ cm}^{-1}$ (P-H bond), 1210 cm^{-1} (P=O bond), and 845 cm^{-1} (P-O-C bond).

The particle size distribution and the morphology of PCellMS were investigated by SEM. The spherical structure of the cellulose phosphate microparticles and the size distribution between $10\text{-}20\text{ }\mu\text{m}$ are shown in Figure 2.

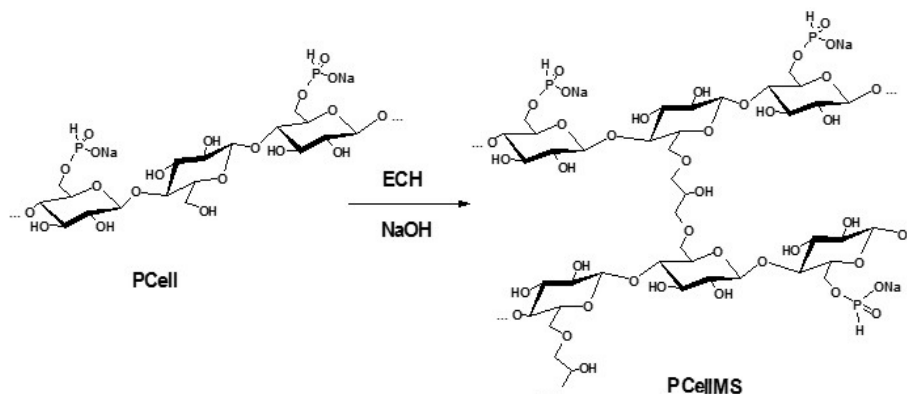
The main characteristics of PCellMS, such as the wrack density, exchange capacity (EC), and particle sizes, are presented in Table 1, and the effect of initial pH solution on the water retention of microspheres is presented in Figure 3.

It can be observed that the initial pH of medium does not influence the water retention rate of PCellMS, the amount of eight grams per gram microspheres remaining constant through the pH domain. This behaviour can be explained by the high degree of cross-linking and by the low value of pK_a of monobasic phosphate groups ($\text{pK}_a=2.4$).²⁰

Dye adsorption

Influence of initial pH and sorbent dosage on dye adsorption

The pH is one of the most important process variables when considering dye adsorption. The effect of the solution pH on the amount of dye adsorbed on PCellMS at equilibrium was investigated varying the initial solution pH in the range of $2.0\text{-}11.0$, at $25\text{ }^\circ\text{C}$ (Fig. 4a), the other parameters being kept constant.



Scheme 1: Synthesis of PCellMS by chemical cross-linking with epichlorohydrin

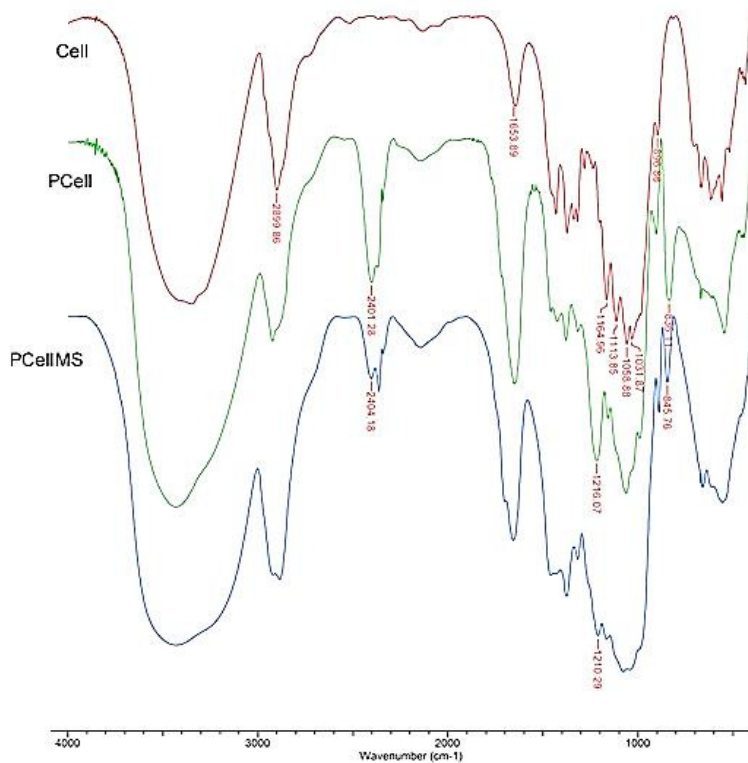


Figure 1: FTIR spectra of parent cellulose, monobasic cellulose phosphate and microparticles based on phosphorylated cellulose

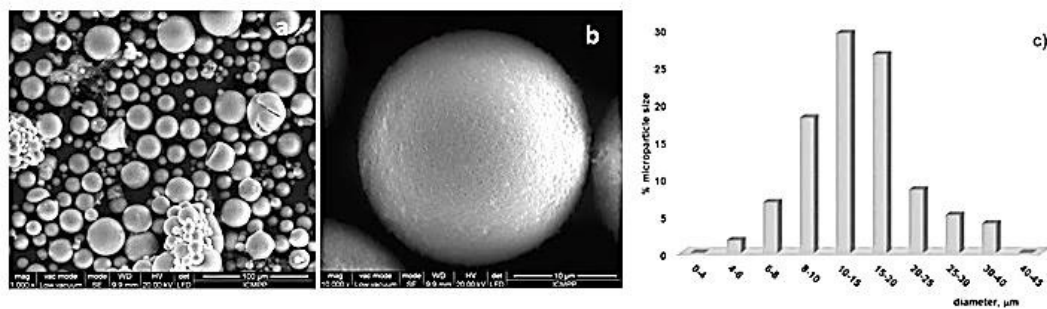


Figure 2: ESEM photographs of PCellMS. General view (a), surface detail (b), and the corresponding size distribution (c)

Table 1
Main characteristics of phosphorylated polysaccharide microspheres^a

Sample code	Wrack density, g/mL	EC, mequi./g	Particle size, μm
PCellMS	0.53 ± 0.02	0.24 ± 0.01	20 - 38

^a The values are the mean of three independent measurements ± SD

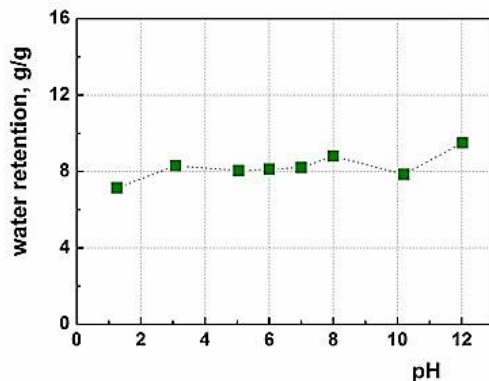


Figure 3: Effect of pH on water retention of PCellMS

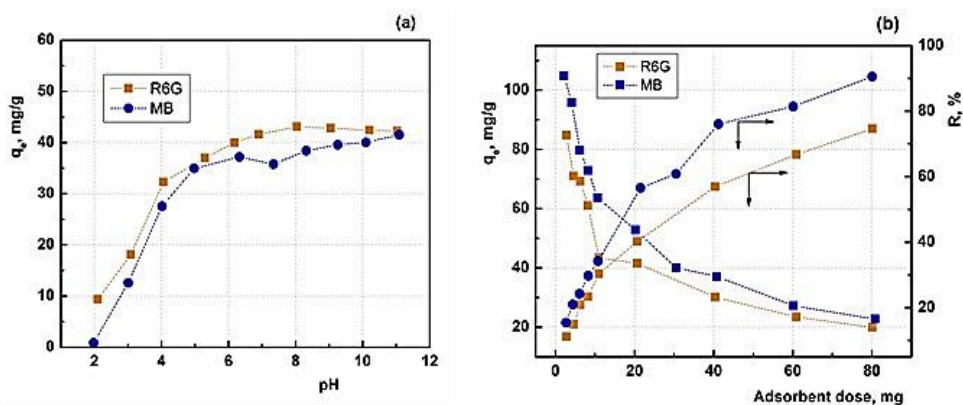


Figure 4: Effect of pH (a) and adsorbent dose (b) on adsorption of dyes, at 25°C (adsorbent dose = 20 mg, [dye] = 100 mg/L, contact time = 48 h)

At pH = 2, the monobasic phosphate groups from the cellulose derivative are in the protonated form and the adsorption of cationic dyes is close to zero, but with the increase of the pH, the anionic groups begin to dissociate and the dye adsorption increases until the pH is around 6. Over this value, the amount of dye adsorption into the microparticles remained almost constant.

In order to study the effect of the adsorbent dosage on dye adsorption, various amounts of PCellMS (2-80 mg) were placed in the dye solutions with a concentration of 100 mg/L. The natural pH of R6G and MB in water was 5.3 and 5.5, respectively. The dye adsorption efficiency increases with the increase of the adsorbent dose (Fig. 4b). In the presence of 80 mg PCellMS, almost complete adsorption (90%) of MB was achieved, while the removal percentage for R6G was of only 70%. This difference can be attributed to a more voluminous structure of R6G compared with MB. Increasing the adsorbent dose, additional adsorbent sites become available

and hence increasing amounts of the dye are removed from the solution.

Equilibrium adsorption

The dye adsorption process is governed by mass transfer from solution to adsorbent, which can be explained mathematically by equilibrium isotherm and kinetic models.²¹⁻²³ The adsorption properties and equilibrium data illustrate how adsorbate molecules interact with the adsorbent and are therefore very important to optimize the use of cellulose phosphate microspheres. Experimental data were examined using several isotherm models (Fig. 5a and b) in order to establish the most appropriate model to design the adsorption of ionic microspheres. The corresponding parameters are listed in Table 2. The shape of the curves indicates isotherms of “L” type, suggesting a progressive saturation of the microspheres.²²

The linearized form of the Langmuir isotherm (Fig. 5c) fits the data measured for both dyes,

over the whole concentration range. The values of correlation coefficients (R^2) were of 0.998 and 0.994 for MB and R6G, respectively (see Table 2). The Langmuir parameter (a_L), known as binding constant, is related to the energy of adsorption, and indicates the affinity or the binding strength of the dye to the adsorbent. The high values of a_L indicate a strong adsorption of the dye on the adsorbent. In our case, the higher value of a_L for MB than a_L of R6G implies a comparatively higher affinity of PCellMS for MB. The good agreement between the experimental

and the calculated values of q_e according to the Langmuir model (Table 2) indicates that the dye forms a monolayer coverage onto the microspheres surface. It was also observed that the value of the adsorption capacity of PCellMS for R6G was higher than for the MB, though the volume of the R6G molecule is higher than the volume of the MB molecule. This behavior could be attributed to the different number of moles adsorbed for each dye into PCellMS: 134 mmol R6G and 150.38 mmol MB per gram of microspheres.²⁴

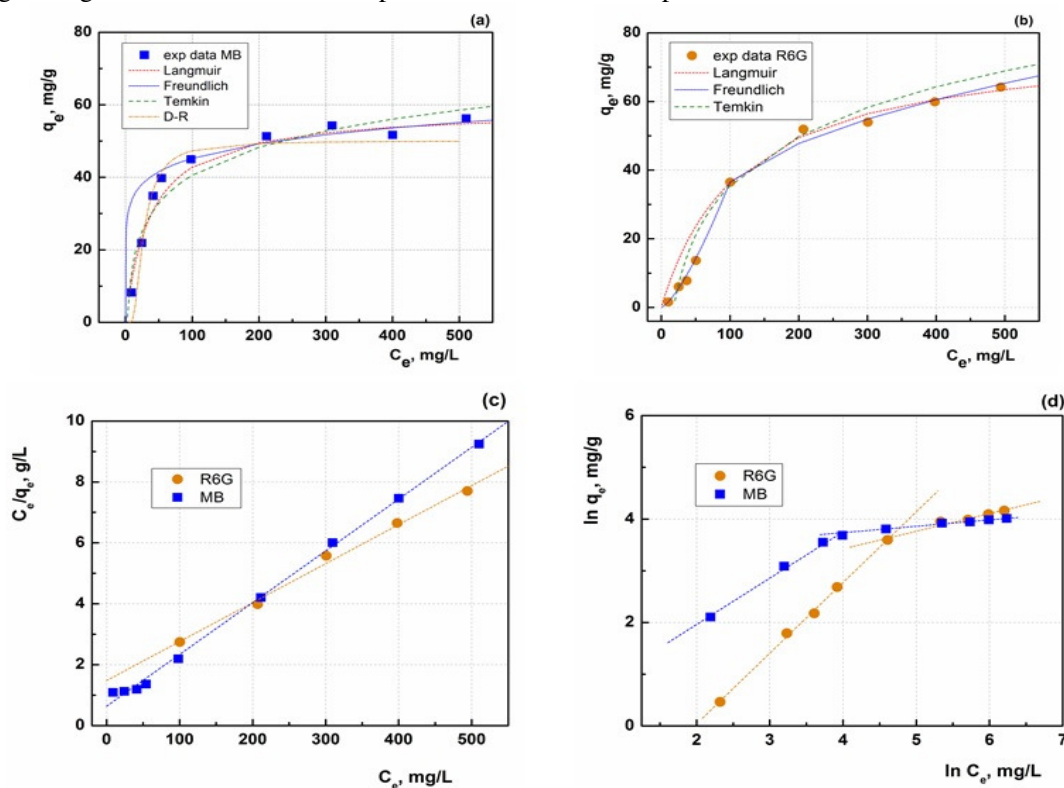


Figure 5: Equilibrium adsorption isotherm of dyes MB (a) and R6G (b) onto PCellMS. Langmuir (c) and Freundlich (d) models describing the adsorption

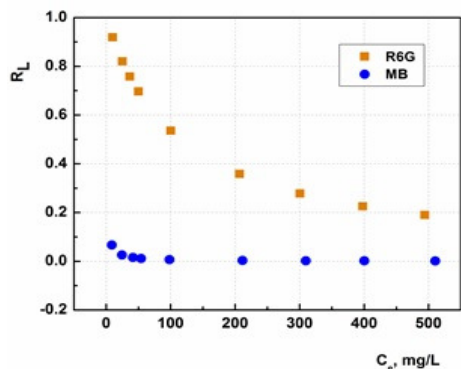


Figure 6: Separation factor (R_L) as a function of initial dye concentration

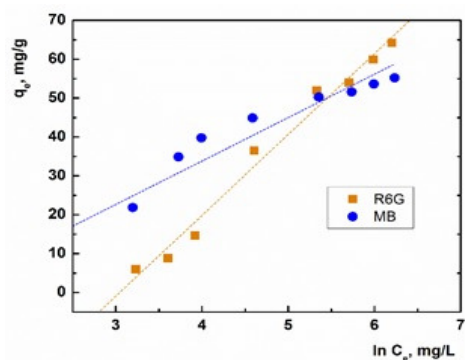


Figure 7: Temkin plot for adsorption of dyes MB and R6G onto PCellMS

Table 2
Langmuir, Freundlich, Temkin and Dubinin-Radushkevich adsorption parameters of PCellMS adsorbent at 25 °C by linear regression models

Isotherm	Parameters	Sample	
		MB	R6G
Langmuir	a_L , L/mg	0.267	0.0086
	K_L , L/g	1.569	0.676
	q_m , mg/g	58.82	78.13
	$q_{e,exp}$, mg/g	56.23	64.19
	R_L	0.0684±0.8073	0.1895±0.9189
	R^2	0.998	0.994
Freundlich	Low concentration		
	K_F , L/mg	1.186	7.541
	n_F	1.116	1.780
	R^2	0.994	0.976
	High concentration		
	K_F , L/mg	25.68	0.000769
Temkin	n_F	8.136	0.3133
	R^2	0.989	0.966
	a_T , L/mg	0.379	0.0476
	b_T , J/mol	222.317	119.331
	R^2	0.934	0.9837
	Dubinin-Radushkevich	q_{DR} , mg/g	49.028
k_{DR} , mol ² /kJ ²		84.411	37.237
E , kJ/mol		0.0769	0.116
R^2		0.963	0.920

Although the exchange capacity of PCellMS was at a low level (EC = 0.24 mequi./g), the q_e values were relatively high due to retention of dyes not only by electrostatic interactions, but also by hydrogen bonds. The adsorption capacity of PCellMS was lower, compared with that of some adsorbents based on anionic cellulose^{8,25} derivatives, but it was still found to be higher than that of other ionic or non-ionic cellulose materials.^{6,9,26} The value of R_L for the adsorption of both dyes was found to decrease with the increase in dye solution concentration (Fig. 6), and the calculated values for both dyes between 0.0665±0.00125 for MB and 0.9189±0.1895 for R6G (Table 2) indicated a favourable dye adsorption process.

By plotting the experimental data using the linear Freundlich equation (7) (Fig. 5d), deviations from linearity were observed, obtaining low values of R^2 . However, when the concentration range was divided into two regions (low and high concentrations) a good fit of results ($R^2 > 0.966$) was observed. The values of Freundlich isotherm parameters are also included in Table 2. This multi-linearity of the isotherm is normally attributed to irregular energy distributions, due to different groups on the

surface, with different levels of activation energies for the range of sorption.^{8,27}

By plotting q_e vs. $\ln C_e$ (Fig. 7) using Temkin model (Eq. 12), the Temkin constants a_T and b_T were determined as intercept and slope (Table 2). The low values of the Temkin adsorption potential, a_T , could indicate a low potential of the PCellMS microspheres, and the values of b_T (0.222-0.119 kJ/mL) suggested a weak interaction between adsorbate (dye) and adsorbent (PCellMS).²⁸

The adsorption data were also fitted with the linearized form of the D-R isotherm model (Eq. 8), and the obtained parameters are presented in Table 2. The values of the free energy of adsorption (E), are limited to 0.0769 and 0.116 kJ/mol for MB and R6D, respectively. Based on these data, it can be concluded that the physical adsorption played a dominating role in the adsorption process of dye adsorption onto the PCellMS.

From the above discussion, in terms of R^2 values, the applicability of the above models for the present experimental data followed approximately the order: i) for MB: Langmuir > Freundlich > Dubinin-Radushkevich > Temkin; ii) for R6G: Langmuir > Temkin > Freundlich > Dubinin-Radushkevich. It is clear that for the

whole concentration range, the equilibrium adsorption data were better explained by the Langmuir isotherm, for both dyes.

Adsorption kinetics

Adsorption kinetics is a vital evaluation element for an adsorption process that depends on the adsorbate-adsorbent interaction and system conditions. The effect of the contact time and the concentration of dye solution on the adsorption kinetics are presented in Figure 8. As expected, the overall trend was the increase of the adsorption in time, becoming constant after 24 hours. The dye adsorption increased with the increasing of initial dye concentration from 100 to 500 mg/L.

In order to evaluate the kinetic mechanism, the experimental data were analysed by several kinetic models: pseudo-first order (Eq. 13), pseudo-second (Eq. 14), intra-particle diffusion (Eq. 15), and Boyd's model (Eq. 16), as shown in Figures 9 and 10. The kinetic parameters estimated from these plots (presented in Table 3) show that the R^2 values are higher (>0.98) for the pseudo-second order kinetic model (for both dyes) than for the pseudo-first order one. This suggested that the adsorption kinetics of dyes on PCellMS microspheres follows the pseudo-second order kinetic model and supports the assumption that the dye adsorption occurs by physisorption.

The intra-particle diffusion model was employed to find the probable dye-adsorption mechanism. It has been reported that if the linear plot of q_t vs $t^{1/2}$ passes through the origin, the

intra-particle diffusion mechanism is considered as a rate-limiting step for the adsorption process; otherwise, the film diffusion process is the predominant mechanism of the adsorption process. Plotting the experimental data according to the intra-particle model (Fig. 10 a and b), the multi-linearity in three regions was observed. The first region is attributed to the diffusion of dyes through the solution to the external surface of microspheres or to the boundary layer diffusion of solute molecules (film diffusion or external mass transfer) with an instantaneous blocking of the available sites on the external surface of microspheres. The second region represents the intra-particle diffusion process, when the dye molecules enter the porous structure of microparticles. The last region, which is the slowest stage, can be attributed to the equilibrium phase, where the adsorption site on the microspheres and the concentration of the dye solution are limited.^{8,29} As shown in Table 3, none of the regions has I values equal to zero, which indicates that these lines do not pass through the origins. This means that the adsorption process occurred by both external diffusion and intra-particle diffusion.³⁰ Boyd's model (Eq. 16) also confirmed these observations, when the Boyd plots did not pass through the origin (Fig. 10 c and d). This suggests, for the present system, that the film diffusion plays a certain role in the rate-limiting process, and the intra-particle diffusion is not the only rate-controlling process in the adsorption of dyes on the PCellMS.

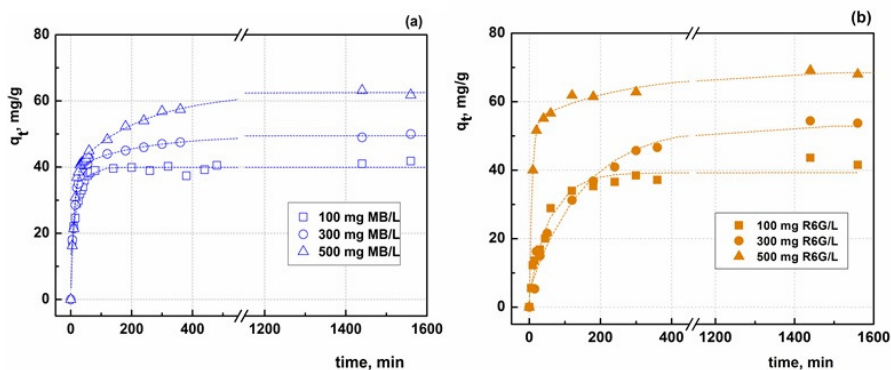


Figure 8: Adsorption kinetics of MB (a) and R6G (b) onto PCellMS microspheres

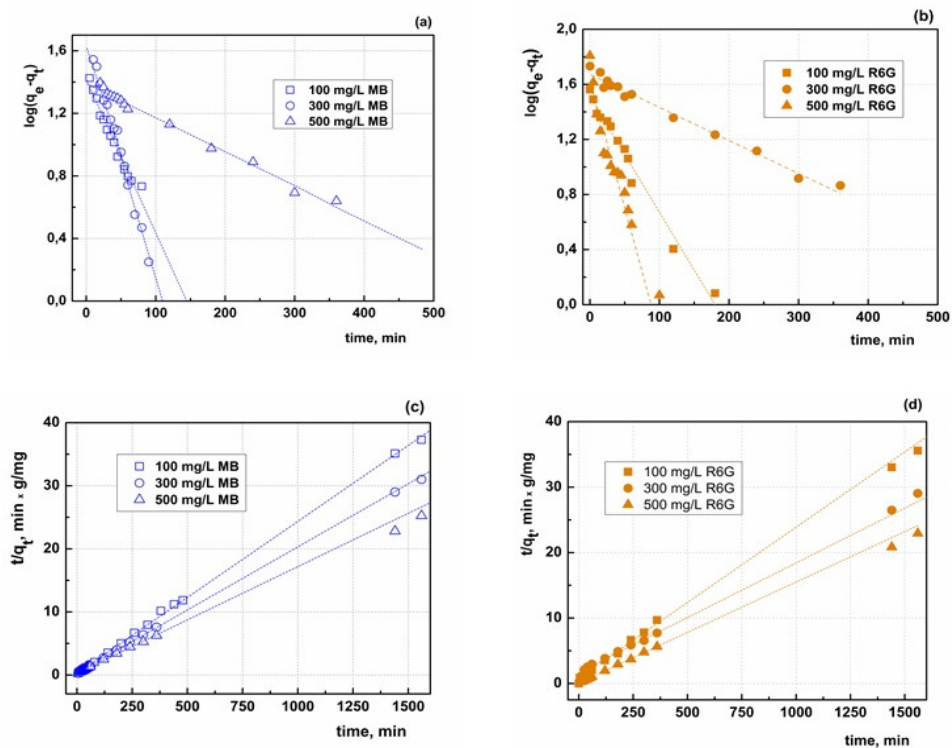


Figure 9: Pseudo-first (a and b) and second order (c and d) plots for the adsorption of MB and R6G on PCellMS microspheres

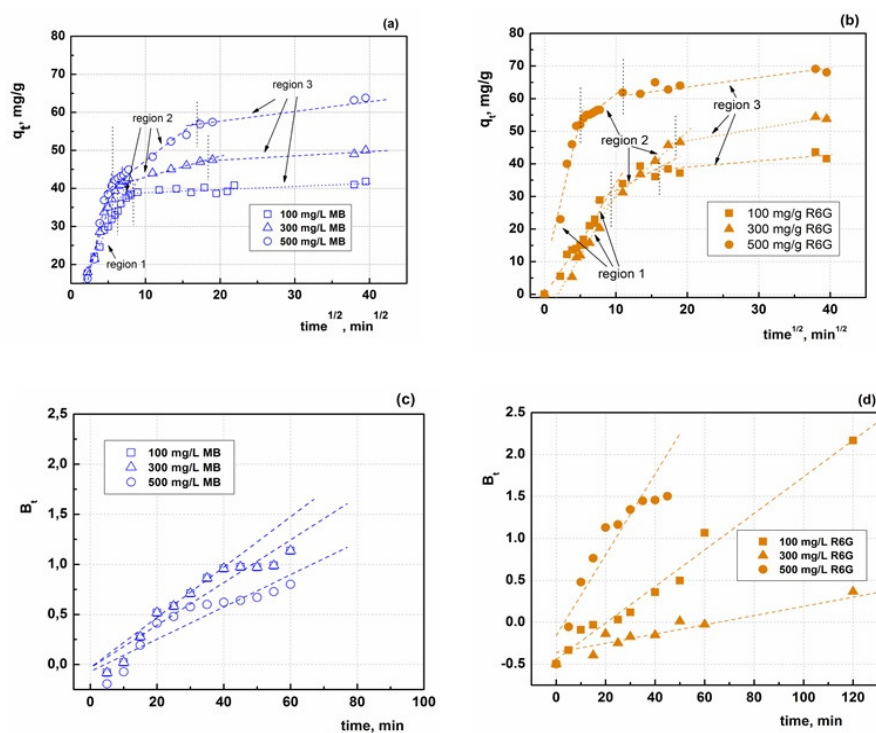


Figure 10: Intra-particle diffusion plot (a and b) and Boyd's plot (c and d) for MB and R6G on PCellMS microspheres

Table 3
Pseudo-first order, pseudo-second, and intra-particle diffusion kinetics for adsorption of acid dyes on PCellMS microparticles

Dye	C_0 , mg/L	Methylene Blue			Rhodamine 6G			
		100	300	500	100	300	500	
Pseudo-first-order	k_1 , min ⁻¹	0.0226	0.0345	0.0051	0.01934	0.00553	0.0396	
	q_e , mg/g	4.122	5.1872	4.0370	4.5303	5.326	4.995	
	R^2	0.964	0.959	0.989	0.9809	0.984	0.918	
Pseudo-second-order	k_2 , g/mg.min ⁻¹	0.00226	0.00129	0.00099	0.000571	0.000161	0.00217	
	q_e , mg/g	41.494	50.00	59.172	43.478	59.880	64.935	
	R^2	0.999	0.995	0.998	0.999	0.993	0.999	
Intra-particle diffusion	Region 1	k_{i1} , g/g.min ^{-1/2}	4.461	5.850	8.789	3.263	3.781	9.188
		I_1 , mg/g	7.848	5.085	-4.176	-0.203	-7.163	7.340
		R^2_1	0.986	0.970	0.970	0.948	0.906	0.895
	Region 2	k_{i2} , g/g.min ^{-1/2}	2.984	0.549	1.531	1.157	2.009	1.721
		I_2 , mg/g	15.330	37.445	31.934	20.318	9.647	44.151
		R^2_2	0.986	0.965	0.979	0.938	0.981	0.979
	Region 3	k_{i3} , g/g.min ^{-1/2}	0.077	0.112	0.256	0.188	0.372	0.295
		I_3 , mg/g	38.392	45.205	52.525	35.255	39.618	57.654
		R^2_3	0.731	0.931	0.947	0.794	0.979	0.798

CONCLUSION

New monobasic cellulose phosphate microspheres were synthesised by chemical cross-linking with ECH using the w/o inverse emulsion technique. Scanning electron microscopy highlighted the spherical shape and 10-20 μm size of the microparticles. The efficiency of the monobasic cellulose phosphate microspheres as adsorbent for the retention of cationic dyes from aqueous solution has been investigated. The adsorption capacity, very low in acidic media, increases with the solution pH, attaining high values at pH = 6, when all the phosphoric groups of the sorbent are dissociated. The Langmuir model fitted to the adsorption data better than the Freundlich model. The shape of the curves indicates isotherms of "L" type, suggesting a progressive saturation of the microspheres. The kinetic adsorption data were in close agreement with the pseudo-second order kinetic model and supports the assumption that the dye adsorption occurs by physic-sorption. Intra-particle and Boyd's models suggested that the intra-particle diffusion was not the only rate-controlling process, and that the film diffusion process also plays some role in the adsorption of dyes on the monobasic cellulose phosphate microspheres.

ACKNOWLEDGEMENTS: This work was supported by a grant of the Romanian National Authority for Scientific Research and Innovation, CNCS – UEFISCDI, project number PN-II-RU-TE-2014-4-0437.

REFERENCES

- ¹ M. T. Yagub, T. K. Sen, S. Afroze and H. M. Ang, *Adv. Colloid Interface Sci.*, **209**, 172 (2014).
- ² G. Crini, *Bioresour. Technol.*, **97**, 1061 (2006).
- ³ G. Crini, *Prog. Polym. Sci.*, **30**, 38 (2005).
- ⁴ C. Pohontu, M. Popa, J. Desbrieres and L. Verestiuc, *Cellulose Chem. Technol.*, **50**, 609 (2016).
- ⁵ L. Ochiuz, M. Hortolomei, I. Stoleriu and M. Bercea, *Cellulose Chem. Technol.*, **50**, 569 (2016).
- ⁶ L. S. Silva, L. C. B. Lima, F. C. Silva, J. M. E. Matos, M. R. M. C. Santos *et al.*, *Chem. Eng. J.*, **218**, 89 (2013).
- ⁷ F. C. Silva, L. C. B. Lima, R. D. S. Bezerra, J. A. Osajima and E. C. S. Filho, in "Cellulose – Fundamental Aspects and Current Trends", edited by M. Poletto and H. L. Ornaghi Jr., InTech., 2015, Chapter 5.
- ⁸ N. K. Goel, V. Kumar, N. Misra and L. Varshney, *Carbohydr. Polym.*, **132**, 444 (2015).
- ⁹ I. A. Udoetok, R. M. Dimmick, L. D. Wilson and J. V. Headley, *Carbohydr. Polym.*, **136**, 329 (2016).
- ¹⁰ S. Hokkanen, A. Bhatnagar and M. Sillanpaa, *Water Res.*, **91**, 156 (2016).
- ¹¹ N. A. El-Kelesh and G. A. Mahmoud, *Cellulose Chem. Technol.*, **49**, 881 (2015).
- ¹² P. L. Granja, L. Pouysegue, M. Petraud, De Jeso, C. Baquey *et al.*, *J. Appl. Polym. Sci.*, **82**, 3341 (2001).
- ¹³ T. Groth and W. Wagenknecht, *Biomaterials*, **22**, 2719 (2001).
- ¹⁴ D. M. Suflet, G. C. Chitanu and V. I. Popa, *React. Funct. Polym.*, **66**, 1240 (2006).
- ¹⁵ K. W. Pepper, D. Reichenberg and D. K. Hale, *J. Am. Chem. Soc.*, **15**, 3129 (1952).
- ¹⁶ K. Y. Foo and B. H. Hameed, *Chem. Eng. J.*, **156**, 2 (2010).

- ¹⁷ A. Gunay, E. Arslankaya and I. Tosun, *J. Hazard. Mater.*, **146**, 362 (2007).
- ¹⁸ G. E. Boyd, A. W. Adamson and L. S. Myers Jr., *J. Am. Chem. Soc.*, **69**, 2836 (1947).
- ¹⁹ Y. S. Ho and G. McKay, *Chem. Eng. J.*, **70**, 115 (1998).
- ²⁰ D. M. Suflet, A. Nicolescu, I. Popescu and G. C. Chitanu, *Carbohydr. Polym.*, **84**, 1176 (2011).
- ²¹ S. J. Allen, G. Mckay and J. F. Porter, *J. Coll. Inter. Sci.*, **280**, 322 (2004).
- ²² G. Limousin, J.-P. Gaudet, L. Charlet, S. Szenknect, V. Barthes *et al.*, *Appl. Geochem.*, **22**, 249 (2007).
- ²³ G. Crini and P.-M. Badot, *Prog. Polym. Sci.*, **33**, 399 (2008).
- ²⁴ I. Popescu and D.M. Suflet, *Polym. Bull.*, **73**, 1283 (2016).
- ²⁵ H. Qiao, Y. Zhou, F. Yu, E. Wang, Y. Min *et al.*, *Chemosphere*, **141**, 297 (2015).
- ²⁶ S. Kumari, D. Mankotia and G. S. Chauhan, *J. Environ. Chem. Eng.*, **4**, 1126 (2016).
- ²⁷ Y. C. Wong, Y. S. Szeto, W. H. Cheung and G. McKay, *Langmuir*, **19**, 7888 (2003).
- ²⁸ X.-J. Hu, J.-S. Wang, Y.-G. Liu, X. Li, G.-M. Zeng *et al.*, *J. Hazard. Mat.*, **185**, 306 (2011).
- ²⁹ W. H. Cheung, Y. S. Szeto and G. McKay, *Bioresour. Technol.*, **98**, 2897 (2007).
- ³⁰ J. Wang, H. B. Li, C. D. Shuang, A. M. Li, C. Wang *et al.*, *Micropor. Mesopor. Mat.*, **210**, 94 (2015).